Boundary layers of aqueous surfactant and block copolymer solutions against hydrophobic and hydrophilic solid surfaces

2005 J. Phys.: Condens. Matter 17 S665

(http://iopscience.iop.org/0953-8984/17/9/023)

INSTITUTE OF PHYSICS PUBLISHING JOURNAL OF PHYSICS: CONDENSED MATTER

J. Phys.: Condens. Matter **17** (2005) S665–S683 doi:10.1088/0953-8984/17/9/023

Boundary layers of aqueous surfactant and block copolymer solutions against hydrophobic and hydrophilic solid surfaces

Roland Steitz[1,2], **Sebastian Schemmel**[1], **Hongwei Shi**[1] **and Gerhard H Findenegg**[1]

[1] Stranski-Laboratorium für Physikalische und Theoretische Chemie, Technische Universität Berlin, Strasse des 17. Juni 112, D-10623 Berlin, Germany
[2] Hahn-Meitner-Institut, SF1, Glienicker Straße 100, D14109 Berlin, Germany

Received 24 November 2004
Published 18 February 2005
Online at stacks.iop.org/JPhysCM/17/S665

Abstract

The boundary layer of aqueous surfactants and amphiphilic triblock copolymers against flat solid surfaces of different degrees of hydrophobicity was investigated by neutron reflectometry (NR), grazing incidence small angle neutron scattering (GISANS) and atomic force microscopy (AFM). Solid substrates of different hydrophobicities were prepared by appropriate surface treatment or by coating silicon wafers with polymer films of different chemical natures. For substrates coated with thin films (20–30 nm) of deuterated poly(styrene) (water contact angle $\theta_w \approx 90°$), neutron reflectivity measurements on the polymer/water interface revealed a water depleted liquid boundary layer of 2–3 nm thickness and a density about 90% of the bulk water density. No pronounced depletion layer was found at the interface of water against a less hydrophobic polyelectrolyte coating ($\theta_w \approx 63°$). It is believed that the observed depletion layer at the hydrophobic polymer/water interface is a precursor of the nanobubbles which have been observed by AFM at this interface.

Decoration of the polymer coatings by adsorbed layers of nonionic C_mE_n surfactants improves their wettability by the aqueous phase at surfactant concentrations well below the critical micellar concentration (CMC) of the surfactant. Here, GISANS experiments conducted on the system $SiO_2/C_8E_4/D_2O$ reveal that there is no preferred lateral organization of the C_8E_4 adsorption layers.

For amphiphilic triblock copolymers (PEO–PPO–PEO) it is found that under equilibrium conditions they form solvent-swollen brushes both at the air/water and the solid/water interface. In the latter case, the brushes transform to uniform, dense layers after extensive rinsing with water and subsequent solvent evaporation. The primary adsorption layers maintain properties of the precursor brushes. In particular, their thickness scales with the number of ethylene oxide units (EO) of the block copolymer. In the case of dip-coating

without subsequent rinsing, surface patterns of the presumably crystalline polymer on top of the primary adsorption layer develop upon drying under controlled conditions. The morphology depends mainly on the nominal surface coverage with the triblock copolymer. Similar morphologies are found on bare and polystyrene-coated silicon substrates, indicating that the surface patterning is mainly driven by segregation forces within the polymer layers and not by interactions with the substrate.

(Some figures in this article are in colour only in the electronic version)

1. Introduction

Wetting phenomena occur at the coexistence of three phases. The equilibrium condition of three-phase contact can be formulated in terms of the interfacial tensions of the three pairs of interfaces involved, namely S/L, S/G and L/G, where S represents a solid substrate, L a liquid phase and G the gas phase coexisting with this liquid phase. Commonly the tension γ_{SG} is greater than γ_{SL} and γ_{LG}, and the wetting behaviour of the S/G interface is characterized by the condition $\gamma_{SG} \leqslant \gamma_{SL} + \gamma_{LG}$, where the inequality corresponds to incomplete wetting and the equality to complete wetting of the S/G interface by phase L. Complete wetting implies that a macroscopically thick layer of phase L will spread at the S/G interface such that this S/G interface is replaced by a sum of S/L and L/G. In the present work we were mainly interested in the structure of the boundary layer of water and of aqueous solutions of amphiphiles against solid substrates of different degrees of hydrophobicity under conditions of complete wetting of the substrate by the liquid phase. We also studied spontaneous and induced structure formation in the boundary layer of water and aqueous solutions of nonionic surfactants and of their polymeric analogues, namely BAB-triblock copolymers, against these solid substrates. The structure of the interface was investigated on a mesoscopic level by several techniques, including neutron and x-ray reflectometry, ellipsometry and atomic force microscopy. Complementary studies on the macroscopic wetting behaviour were conducted by measuring the contact angles of the aqueous surfactant solutions against the solid substrates in air.

The substrates used in this work were silicon single crystals having a native silicon oxide surface layer (SiO_x, layer thickness $d \approx 1.5$ nm). Substrates with hydrophobic surfaces were obtained by coating the silicon blocks with a polymer film (layer thickness $d \approx 30$ nm) of different chemical composition and hydrophobicity. After thorough cleaning as described elsewhere [1] uniform coatings of very low surface roughness ($\sigma \leqslant 0.5$ nm) were achieved in a reproducible way (figure 1).

This paper reports novel results but also contains short review sections with the results of preceding studies, with brief introductory remarks where appropriate. Paragraphs in which new results are presented are indicated by the word 'results' in the respective heading.

2. Plain interfaces

2.1. Polystyrene films against water

The interface of water against an inert polymer is commonly conceived as a case of a simple S/L interface. We have investigated the interface formed by heavy water (D_2O) and fully deuterated polystyrene films (d-PS) on a silicon single crystal block using neutron reflectometry and

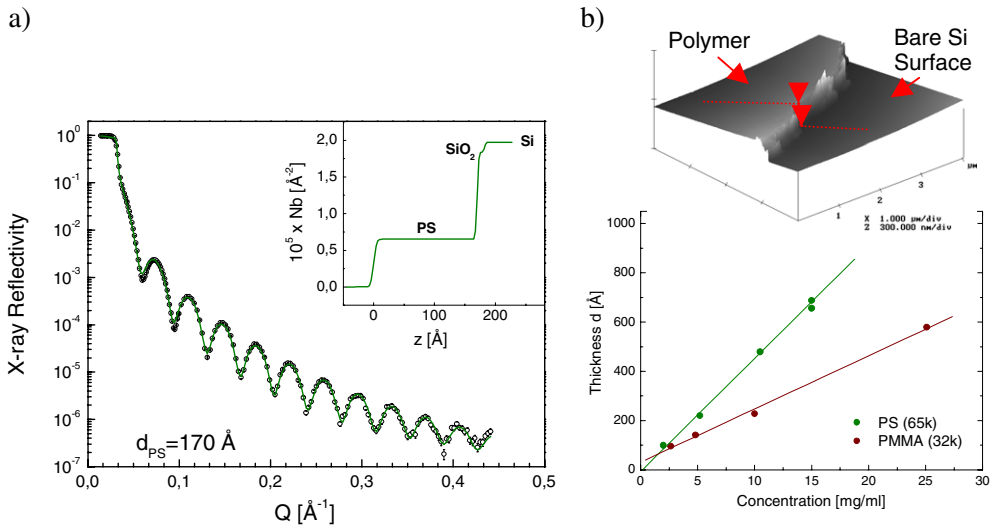

Figure 1. Spin-coated polymer films on top of silicon single crystals characterized by x-ray reflectivity (left) and AFM (right, top). The film thickness (as extracted from the reflectivity experiments) scales linear with polymer concentration of the spin coating solution in toluene at a constant spin speed of 3500 rpm (bottom right).

atomic force microscopy [1]. A systematic study of this system revealed that water is depleted in the boundary layer of the liquid phase against the hydrophobic substrate (see figure 2). From the combined results of the NR and AFM measurements we conjectured that the water-depleted layer at the interface represented the precursor layer of submicroscopic gas bubbles that were recently observed by Tyrrell and Attard [2] on related surfaces. We confirmed the existence of such gas nanobubbles in our d-PS/D_2O system by AFM measurements (see figure 3). The thickness of the precursor gas layer as determined by neutron reflectometry was 2–5 nm, depending on the level of air saturation of the water sample and on the time elapsed after contacting it with the hydrophobic surface [1].

Our findings are consistent with results of other groups [3, 4] which also revealed water depletion layers at the interface against organic surfaces. The experimental results may be discussed in the general context of wetting and drying transitions [5] where the depletion of water is seen as a (weak) dewetting of the aqueous phase from the hydrophobic walls (d-PS coating, $C_{36}H_{74}$ monolayer). It is interesting to note that the water depletion effect is observed for surfaces of different degrees of hydrophobicity, as the advancing macroscopic contact angle of water, θ_w, at our d-PS coatings is $90° \pm 2°$, but only $63° \pm 2°$ for self-assembled monolayers of hydroxy tri(ethylene glycol) terminated undecylthiolate on gold surfaces studied by Schwendel *et al* [4]. Similar effects pointing at water depleted boundary regions have been reported by Ishida and co-workers from force–distance measurements on interacting hydrophobic surfaces in aqueous solutions [6]: Hydrophobic octadecyl trichlorosilane (OTS)-coated silica surfaces ($\theta_w = 90°$) in water and less hydrophobic STAC coated silica surfaces ($\theta_w = 40°$) in STAC (stearyl trimethyl ammonium chloride) solution both showed attractive interaction upon mutual approach. Strong and longer-ranged interactions ($\sim$20 nm) were found for the OTS-coated surfaces, while weak and shorter-ranged interactions ($<$5 nm) were observed in the case of the STAC-coated surfaces. From these findings the authors concluded that hydrophobic interactions become dominant and will cause a dewetting of the aqueous phase from the substrate if the water contact angle exceeds a value of about 40°.

2.2. Results for polyelectrolyte films against water

In order to test the conjectured effect of hydrophobicity of the polymer surface on the appearance of a depletion layer of water at the water/polymer interface we prepared polyelectrolyte multilayers of deuterated poly(styrene sulfonate) (d-PSS) and poly(allyl hydrochloride) (PAH) on silicon single crystal blocks by the layer-by-layer deposition technique [7], using a layer of branched poly(ethylene-imine) (PEI) as a contact layer. The individual layers were formed by dip-coating from 0.02 mol l^{-1} (monomer) solutions of d-PSS, PAH and PEI (the latter two containing 1 M NaCl). Two substrates of different water contact angle were prepared for these studies: Si/PEI/(d-PSS/PAH)$_6$ ($\theta_w = 63° \pm 3°$), and Si/PEI/(d-PSS/PAH)$_6$/d-PSS ($\theta_w = 37° \pm 2°$). NR measurements were performed as described earlier [1], using a liquid flow cell, which consists of a Teflon trough and the polyelectrolyte-coated silicon block, through which the neutron beam is transmitted to and reflected from the interface.

As in our earlier study with d-PS/D_2O (figure 2) the existence of a water-depleted boundary layer can be deduced from the appearance of Kiessig oscillations in the reflectivity curve if the polymer film and the water phase have the same scattering length density (SLD). Since the polyelectrolyte multilayers are known to absorb substantial amounts of water [8, 9], NR measurements were made for a series of D_2O/H_2O mixtures of different SLDs, and the SLD and thickness of the polyelectrolyte film (28–30 nm) was extracted from fits to the spectra (figure 4(a)). Figure 4(b) shows the SLD of the PAH-terminated polyelectrolyte film as a function of the SLD of the D_2O/H_2O water phase. The match point of the SLD of film and water, obtained by a linear fit to the data, yielded Nb $= 5.03 \times 10^{-6}$ Å^{-2}. The characteristic oscillations in the reflectivity curves ('Kiessig fringes') caused by the interference of neutrons reflected at the silicon/film and the film/water interface, respectively, are almost completely suppressed at this contrast match point (figure 4(a), middle). Similar results were obtained for the d-PSS terminated films[3]. These findings not only indicate that the polyelectrolyte coating is contrast matched by the water phase, but also that there exists no significant depletion layer of water at the polyelectrolyte/liquid interface. At least it is safe to say that at interfaces of water against the (relatively hydrophilic) polyelectrolyte films such a depletion layer is much less pronounced than observed at the hydrophobic d-PS/water interface.

Incidentally, the advancing contact angle of water on the PAH-terminated polyelectrolyte multilayers studied in this work was equal within experimental error to that on the self-assembled monolayers (SAMs) studied in [4]. Nevertheless, the wetting behaviour of these two substrates appears to be quite different. While the water-sorbing polyelectrolyte coatings cause no depletion of water in the boundary, pronounced water depletion is occurring in the boundary layer against the SAMs. This finding indicates that the water contact angle cannot be taken as an unambiguous indicator of the onset of a drying transition of water at hydrophobic surfaces. Apparently our knowledge of such 'simple' interfaces is far from complete and further experimental and theoretical work has to be conducted to gain a better understanding.

3. Interfaces with adsorbed surfactant layers

It is generally accepted that the wetting of hydrophobic surfaces by water can be strongly changed by the adsorption of surfactants. As illustrated in figure 5, the contact angle of water (D_2O) on silicon wafers spin-coated with a thin polystyrene (PS) or poly(methylmethacrylate) (PMMA) layer exhibits a characteristic dependence on the concentration of nonionic surfactants of the oligo(ethyleneglycol) mono-*n*-alkyl ether (C_mE_n) family added to the

[3] A detailed analysis of the data is currently under way.

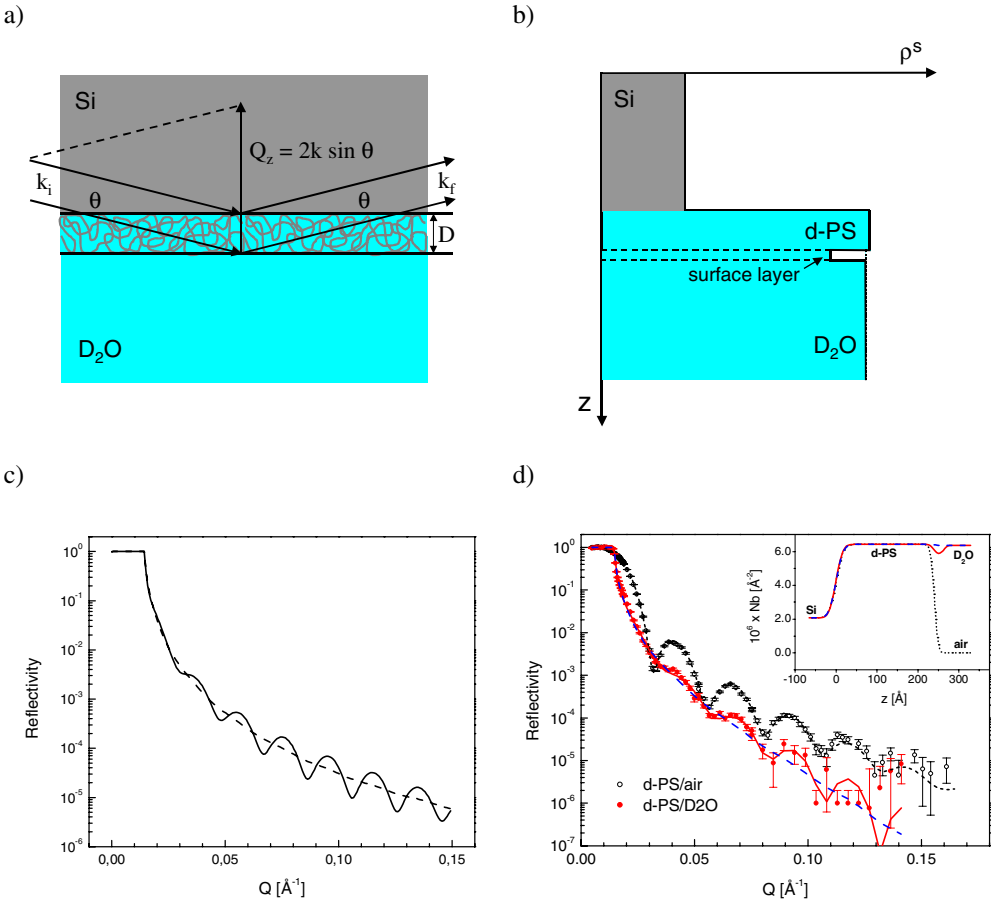

Figure 2. Scattering geometry (a), schematic scattering length density profiles (b) and expected reflectivity curves (c) of the neutron reflectivity experiments. The incident neutrons access the polymer/water interface through the silicon block (Si). As the SLD of the d-PS film almost matches that of pure liquid D_2O, the d-PS/D_2O interface is almost invisible for neutrons, and the reflectivity arises predominantly from the Si/d-PS interface, dashed curve in (c). The existence of a thin depletion layer at the d-PS/D_2O interface causes a local minimum in the SLD. The interference of neutrons scattered at the outer and inner interface of the film gives rise to pronounced Kiessig oscillations, full curve (c). Experimental neutron reflectivity curves of a typical d-PS coating against air, open symbols, and D_2O, solid symbols, (d). Although the scattering length densities of the polymer coating and that of D_2O closely match, see the inset, there is nonvanishing contrast at the d-PS/D_2O interface which causes the pronounced Kiessig oscillations in the experimental reflectivity curve against the liquid phase. This contrast stems from the 2.6 nm thick depletion layer of 9% reduced bulk water density as shown by the solid line in the inset which is the best fit to the experimental data.

aqueous phase. At surfactant concentrations c_S well below the critical micelle concentration (CMC), namely $c_S/\mathrm{CMC} < 0.3$, the contact angle decreases weakly and nearly linearly with the logarithm of c_S, from 90° to about 60° at the PS surface, and from 70° to about 50° at the PMMA surface. At higher concentrations, in the range $0.3 < c_S/\mathrm{CMC} < 0.6$, a much steeper decrease of the contact angle to values less than 10° occurs and eventually the substrate is completely wetted by the surfactant solution at $c_S/\mathrm{CMC} > 0.6$. This characteristic S-shape dependence of the contact angle on $\ln(c_S/\mathrm{CMC})$ is found for both surfactants, C_8E_4 and $C_{10}E_4$,

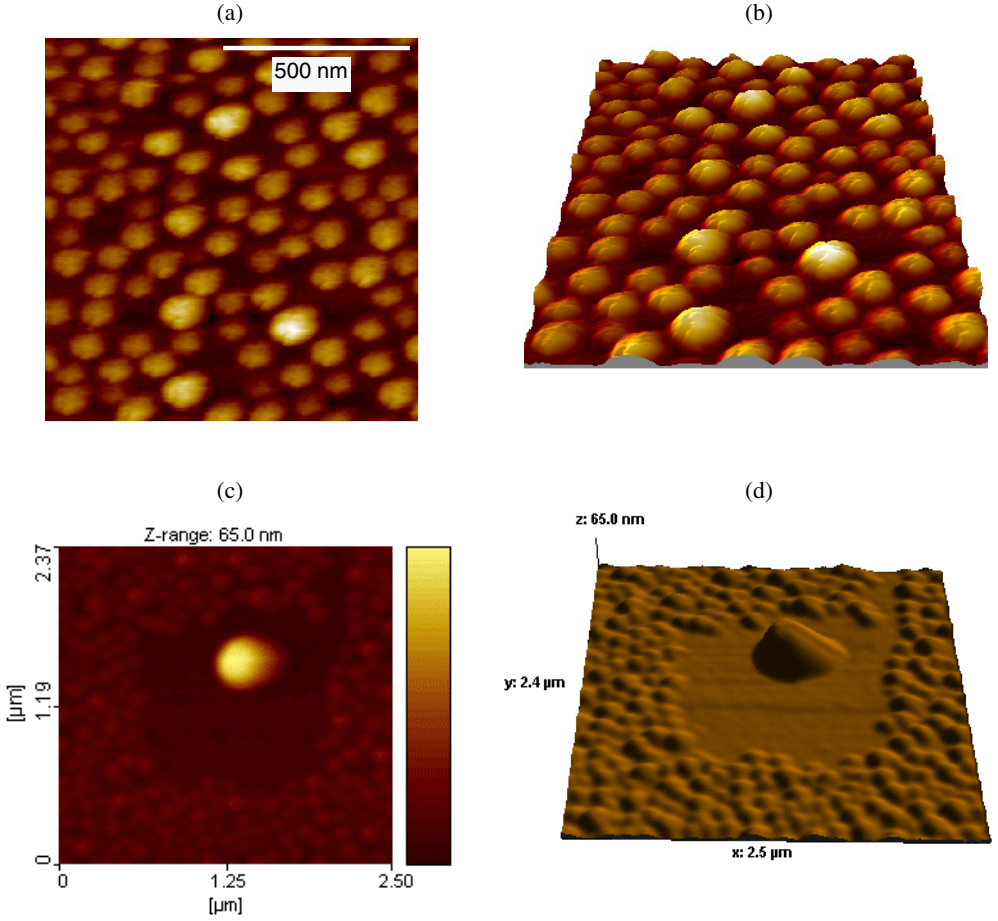

Figure 3. Tapping mode topology image of nanobubbles on a 1 μm square of the surface of a d-PS coated silicon substrate in distilled water (a), and result of a manipulation of the nanobubbles with the AFM tip, by which several nanobubbles have coalesced into one bigger object (c). Images (b) and (d) are 3D projections of the topology images (a) and (c). Note that the lateral dimensions and height are shown on different scales. Please note further that the AFM without tip deconvolution does not offer a proper method to draw conclusions about shapes. This is even more true for highly deformable objects like gas bubbles. Reprinted with permission from [1]. Copyright (2003) American Chemical Society.

on both polymer coatings. Closer inspection of figure 5 shows, however, that the contact angles of the $C_{10}E_4$ solutions are generally somewhat greater than those of the C_8E_4 solutions at the same relative concentration c_S/CMC, which implies that the wetting behaviour does not scale quantitatively with the CMC of the bulk solution. This may be taken as indirect evidence that the structure of the adsorption layer of the two surfactants at their respective CMCs is somewhat different, as the contact angle is expected to depend primarily on the microscopic structure of the adsorption layer at the solid/liquid interface.

Lu and coworkers have shown that neutron reflectometry is a powerful technique for determining the microscopic structure of adsorbed surfactant layers at solid/liquid interfaces [10]. We have used a high-resolution neutron reflectometry technique to study the interface between the aqueous surfactant solutions and polymer-coated silicon blocks coated with polymer layers of 250 Å thickness and an rms roughness of less than 10 Å.

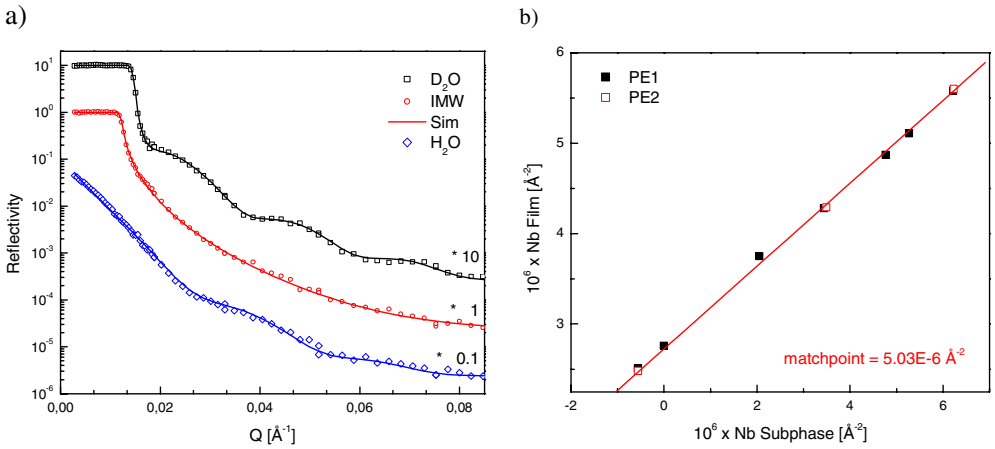

Figure 4. (a) Neutron reflectivity from the interface of a PAH-terminated polyelectrolyte film against D_2O/H_2O mixtures of different scattering length densities, Nb. Solid lines are fits to the data except the solid line labelled 'Sim' which is the calculated reflectivity curve for perfect match of polyelecrolyte layer and adjacent bulk water subphase IMW (index-matched water). (b) Plot of the SLD of the PAH-terminated films, Nb Film, as a function of the SLD of the water fronting, Nb Subphase, and linear fit to the data.

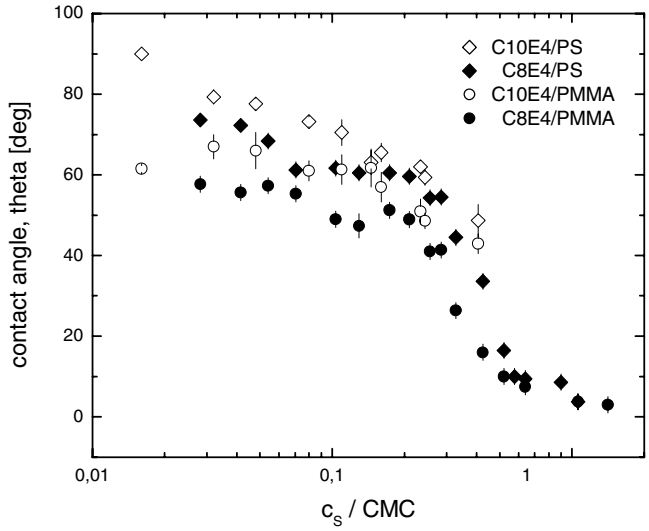

Figure 5. Plot of the advancing contact angle of dilute aqueous solutions of $C_{10}E_4$ and C_8E_4 against PS and PMMA substrates, respectively, versus reduced surfactant concentration c_S/CMC. The CMC of $C_{10}E_4$ in D_2O is 0.75 ± 0.01 mmol l^{-1}; that of C_8E_4 in D_2O is 6.1 ± 0.01 mmol l^{-1}.

3.1. Results for the PMMA/C_8E_4 solution interface

Figure 6 shows a series of neutron reflectivity spectra obtained from the Si/PMMA/liquid interface at room temperature together with model fits to the data. The concentration of the surfactant C_8E_4 in D_2O was varied from values below its CMC (6.1 mmol l^{-1}) to values slightly above the CMC. From the oscillations in the spectrum of the reference system Si/PMMA/D_2O (figure 6, uppermost spectrum) and quantitative model fitting, the thickness

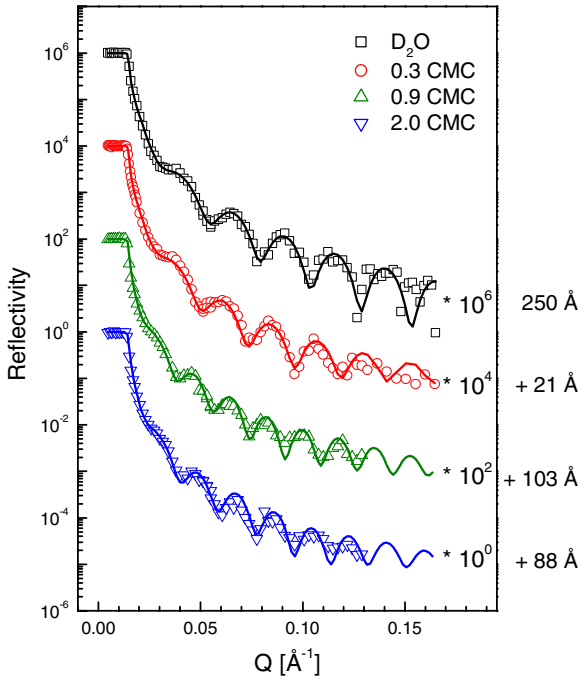

Figure 6. Neutron reflectivity from the interface Si/PMMA/C_8E_4 in D_2O. Top curve: reference spectrum of the plain Si/PMMA/D_2O interface. Solid curves are best box-model fits to the data. For details see the text.

L and scattering length density of the PMMA film were derived, namely $d = 246 \pm 3$ Å and $\mathrm{Nb} = (1.65 \pm 0.13) \times 10^{-6}$ Å^{-2}. The latter value is significantly greater than the SLD of bulk PMMA ($\mathrm{Nb} = 1.03 \times 10^{-6}$ Å^{-2}) [11], indicating that a significant amount (about 11 vol%) of D_2O is incorporated in the polymer layer. When pure water (D_2O) is replaced by a solution of 2 mmol l^{-1} C_8E_4 in D_2O (0.33 CMC) the positions of the minima of the Kiessig oscillations are shifted to smaller momentum transfer Q and the distance between adjacent minima is reduced. These changes in the spectrum indicate the formation of a stable adsorbed film of C_8E_4 at the PMMA surface, having a thickness of 21 ± 4 Å and an SLD of $\mathrm{Nb} = (1.89 \pm 0.30) \times 10^{-6}$ Å^{-2}, which implies that the adsorbed film was composed of 72 vol% C_8E_4 and 28 vol% D_2O. This experimental value of the thickness is slightly smaller than the length of the fully extended C_8E_4 molecule (25 Å), which suggests that the adsorbed surfactant layer is either a (weakly tilted) monolayer or a strongly interdigitated bilayer.

On increasing the bulk surfactant concentration from 0.33 CMC (2 mmol l^{-1}) to 0.90 CMC (5.5 mmol l^{-1}) the thickness of the adsorption layer was found to increase with time, from an initial value of 53 ± 3 Å to a stable value of 103 ± 5 Å after 18 h. The SLD of the ad-layer was $(1.93 \pm 0.10) \times 10^{-6}$ Å^{-2}, nearly unaffected by the growth in the layer thickness. When the bulk surfactant concentration was further increased to a value of 2 CMC (12.3 mmol l^{-1}) a shrinkage of the ad-layer thickness to a value of 85 ± 5 Å was derived from the observed shift of the minima positions of the Kiessig fringes to larger Q (see figure 6, bottom curve).

The adsorption layer of C_8E_4 at the PMMA/D_2O interface could not be removed by repeated exchange of the liquid volume of the sample cell with pure D_2O, but a stable adsorption layer of 55 ± 5 Å thickness and a scattering length density of $(1.86 \pm 0.12) \times 10^{-6}$ Å^{-2} remained after the solvent replacement (spectrum not shown in figure 6).

3.2. Results for the PS/C_8E_4 solution interface

Neutron reflectivity measurements similar to those outlined in section 3.1 were also performed on silicon blocks spin-coated by a thin polystyrene film ($d = 250 \pm 3$ Å, and Nb = $(1.97 \pm 0.13) \times 10^{-6}$ Å^{-2}).[4] It was found that already in rather dilute solution of the surfactant C_8E_4 (0.5 mmol l^{-1} or of 0.08 CMC) the polymer surface was covered by a condensed adsorption layer of 24 ± 2 Å layer thickness, which agrees well the length of the fully extended C_8E_4 molecule (25 Å), and thus suggests a monolayer type adsorption layer.

As in the case of PMMA coatings, the thickness of the adsorbed surfactant layer on the PS coating was found to increase with increasing bulk surfactant concentration. When the 0.5 mmol l^{-1} solution was replaced by a 2 mmol l^{-1} solution, a condensed ad-layer of C_8E_4 of 53 ± 3 Å thickness was formed at the PS surface, and the thickness of the layer increased to 68 Å after a period of 20 h. It is remarkable that the thickness of the C_8E_4 adsorbed film at the PS/water interface is significantly greater than at the interface of the more hydrophilic PMMA against water, where a film of only 22 Å thickness was observed for the same bulk surfactant concentration.

Pronounced time-dependent changes in the reflectivity curve of the Si/PS/solution interface were observed at a bulk surfactant concentration of 5.5 mmol l^{-1} (0.9 CMC). The thickness of the C_8E_4 adsorption layer as derived from the reflectivity curves changed from 100 to 200 Å during a period of 48 h after replacing the 2 mmol l^{-1} solution by the 5.5 mmol l^{-1} solution of C_8E_4. This change was indicated by the shift of the minimum positions of the Kiessig oscillations in the reflectivity spectra (not shown). Simultaneously, the amplitude of the oscillations decreased significantly, indicating that an increasing volume fraction of water was incorporated in the boundary layer. After 48 h the oscillations in the reflectivity curves had almost vanished. We attribute these findings to a gradual peeling-off of parts of the PS film from the silicon substrate at this surfactant concentration. This supposition was supported by a subsequent x-ray reflectivity measurement of the Si/PS substrate in air which did not indicate the existence of any distinct surface coating anymore. Further experiments are necessary to reproduce and to clarify these findings.

Figure 7 summarizes the results of the adsorption study of C_8E_4 at the PMMA and PS surfaces in terms of measured adsorption layer thickness and extracted adsorbed amount [12]. At the surface of the relatively hydrophilic PMMA coating the adsorption behaviour of C_8E_4 shows similarities with that observed at hydrophilic silica by thermodynamic methods [13], namely, a low affinity adsorption region at low surfactant concentrations and a build-up of a condensed adsorption layer close to the bulk CMC. In contrast to this adsorption behaviour on hydrophilic substrates, the adsorption of C_8E_4 at the surface of the hydrophobic PS coating exhibits strongly time-dependent precipitation of surfactant molecules at the substrate surface well below the bulk CMC.

Closer inspection of figure 7(a) indicates that the adsorption layers of C_8E_4 on PS and PMMA build up with distinct jumps in thickness, namely from 20 to 70 Å and 120 Å. Recalling that the length of a fully extended C_8E_4 molecule is 25 Å and thus the diameter of a C_8E_4 micelle is of the order of 50 Å [14], the time-dependent ad-layer formation beyond monolayer coverage (i.e. beyond formation of a first adsorbed layer of 20 Å thickness) may proceed by the formation of a first (+50 Å) and subsequently a second layer of surface micelles (+50 Å), as sketched in the right panel of figure 7.

[4] This value is larger than the scattering length density of the film against air ($(0.95 \pm 0.10) \times 10^{-6}$ Å^{-2}) and larger than the scattering length density of bulk PS (1.35×10^{-6} Å^{-2}) [11] and indicates a D_2O content of 19%, most likely in voids of the polymer film.

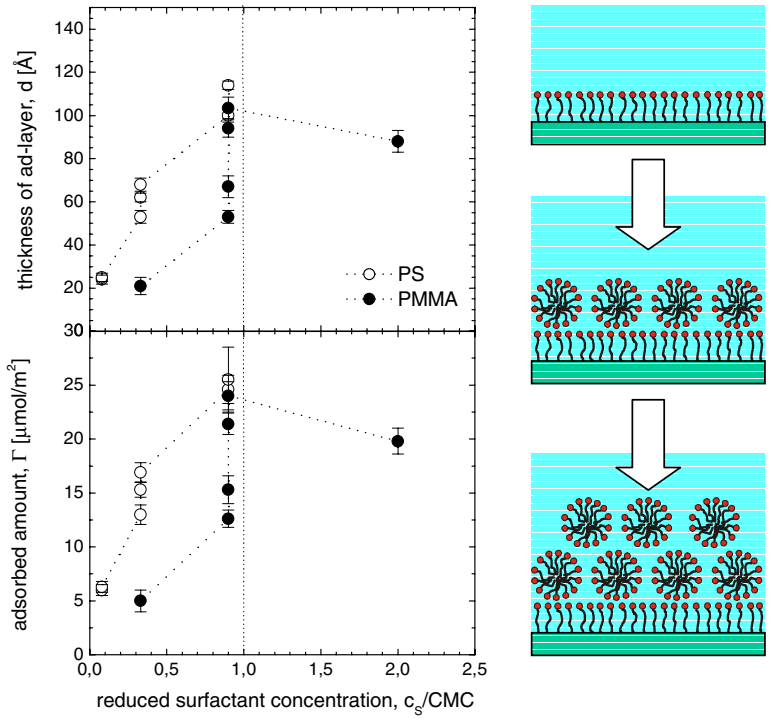

Figure 7. Adsorption of C_8E_4 to PS and PMMA as revealed by neutron reflectometry. Left panel: thickness and adsorbed amount of C_8E_4 in the ad-layer at the PS (open symbols) and PMMA surface (solid symbols) as a function of reduced surfactant concentration and time. Right panel: schematic diagram of ad-layer build-up beyond monolayer thickness. For details see the text.

3.3. $C_{10}E_4$ at PS and PMMA surfaces

To investigate the influence of the hydrophobicity of surfactants on their adsorption at the polymer/water interfaces we have compared two members of the C_mE_n family, namely C_8E_4 and $C_{10}E_4$. As $C_{10}E_4$ is more hydrophobic than C_8E_4, the upper miscibility curve of the $C_{10}E_4$ + D_2O system extends to lower temperatures than that of the C_8E_4 + D_2O system. Significant differences were found in the adsorption of the two surfactants onto PS and PMMA coated surfaces. The adsorption of $C_{10}E_4$ to the PMMA surface at 16 °C (i.e., only about 1 K below the lower critical solution temperature) leads to a layer of 21 Å thickness and surfactant volume fraction 0.63 ± 0.08 over the entire concentration range studied ($0.33 < c_S/\mathrm{CMC} < 4.50$). Experiments above the CMC showed that the adsorption of the surfactant on PMMA is reversible. On the more hydrophobic PS substrate an adsorption layer of 11 Å thickness and surfactant volume fraction 0.53 ± 0.08 was found at the lowest experimental concentration (0.1 CMC). As the surfactant concentration was gradually raised, the thickness of the adsorbed layer increased to 40 Å at 1.20 CMC, with a nearly constant surfactant volume fraction in the layer (0.75 ± 0.03) above a concentration of 0.3 CMC. Experiments above the CMC revealed that a surfactant layer of 18 Å thickness was adsorbed irreversibly to the PS surface [12].

From these studies we conclude that in the regime of low surfactant concentrations the chemical nature of the substrate (PS or PMMA) determines the onset, growth and stability of the adsorption layer of the surfactant. The chemical nature of the surfactant molecules

influences thickness and organization of the ad-layer: although $C_{10}E_4$ and C_8E_4 differ by only two methylene units in the hydrophobic chain, much thicker adsorption layers were found for the shorter molecule C_8E_4 (up to four times the thickness of the corresponding $C_{10}E_4$ adsorption layer) at PS and PMMA substrates. This finding suggests a pronounced difference in the internal molecular organization of the ad-layers [15].

3.4. Lateral structuring of the C_8E_4 adsorption layer at the silicon/liquid interface

The structure of surfactant adsorbed layers at solid/liquid interfaces is determined by a delicate balance of adsorption and self-assembly forces. As already discussed earlier in this chapter, surfactant monolayers or bilayers are commonly formed at the interface, and from the NR measurements we know that surfactant adsorption layers contain between 20 and 40 vol% water [12]. Although NR with selectively deuterated surfactants can provide details of the molecular arrangement in complete (saturated) adsorbed layers, neither ellipsometry [16] nor NR is sensitive to the lateral structure of the adsorbed layer in the regime below full coverage. In particular, the lateral structure of the adsorbed layer of nonionic surfactants on hydrophilic silica (e.g., formation of small surface micelles or large bilayer patches) has remained an open question.

We addressed this question by grazing-incidence small angle neutron scattering [17] measurements on the interface of a hydrophilic silicon substrate against aqueous solutions of C_8E_4 in D_2O at a fixed surfactant concentration of 0.8 CMC [18]. In this concentration range the adsorption isotherms of C_8E_4 are strongly temperature dependent. Specifically, at the chosen surfactant concentration c_s/CMC $= 0.8$, the relative surface concentration of the surfactant is less than 5% of full coverage at 5 °C, but about 50% of full coverage at 25 °C, and nearly 100% of full coverage at 45 °C [19].

The GISANS experiments were performed at beamline D22 of ILL, Grenoble (France), at a wavelength of 0.6 nm, using our home-built flow cell [20] mounted on the two-circle goniometer with z-translation to properly align the solid/liquid interface with respect to the incoming beam. At a fixed angle of incidence ($\alpha_i = 1.55°$) we recorded the specular and off-specular scattered intensity through the silicon backing, using a two-dimensional detector at exit angles α_f (X detector channels) and out-of-plane angles ψ (Y detector channels) at a distance of 4 m from the sample. The beam size in and out of the plane of reflection was set by cross slits on the incident side.

Figure 8 shows a sketch of the experimental set-up together with a contour plot of the scattered intensity in the Q_yQ_z plane resulting from the surfactant adsorbed layer at the solid/liquid interface at 20 °C. Contrary to expectation, no pronounced off-specular peaks are visible. This is direct evidence that no laterally ordered surfactant aggregates (surface micelles) exist at the interface at length in the range 5–320 nm. However, the off-specular diffuse scattering parallel to the solid/liquid interface (i.e. parallel to the sample horizon) exhibits a pronounced dependence on the sample temperature (figure 9). At low temperatures (14 °C and below) there is negligible contribution from the diffuse scattering to the total scattered intensity (<10%). Negligible diffuse scattering is also observed at high temperatures (31 °C and above). This diminishing contribution of the off-specular scattering from the substrate surface indicates a vanishing contrast at the interface for the impinging neutrons. Whereas at low temperatures this is due to the very low concentration of adsorbed surfactant, at high temperature the contrast vanishes due to the formation of a nearly uniform adsorption layer. The pronounced diffuse scattering at intermediate temperatures (between 17 and 28 °C) results from in-plane fluctuations of the scattering length density which are attributed to surface aggregates of the (nondeuterated) surfactant C_8E_4 embedded in the matrix of liquid D_2O.

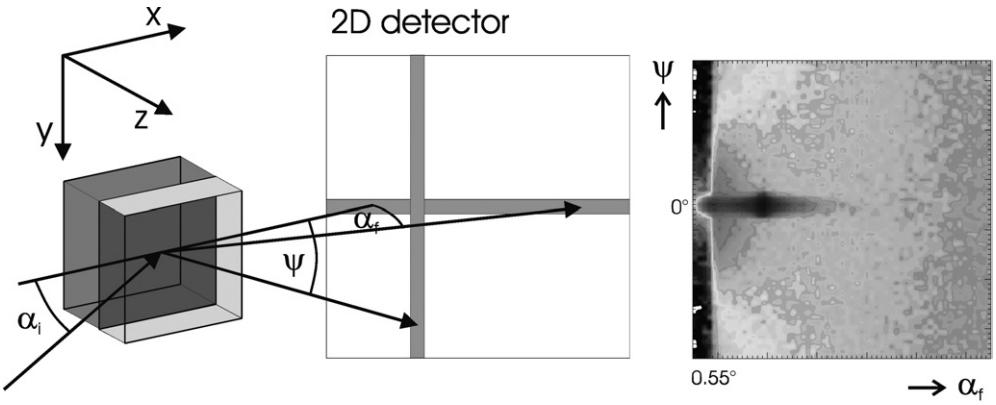

Figure 8. Schematic drawing of the experimental set-up together with one contour plot of a typical intensity distribution at 20 °C. The solid/liquid interface (dark grey) is vertically placed. The angle of incidence is denoted with α_i, the exit angle with α_f and the out-of-plane angle with ψ. The specular reflected beam at $\psi = 0°$ is visible as a dark grey spot at α_f. For data evaluation horizontal and vertical slices (marked in grey) are taken. After: Müller-Buschbaum *et al* [17]. Note that the intensity scale is inverted below $\alpha_f = 0.55°$.

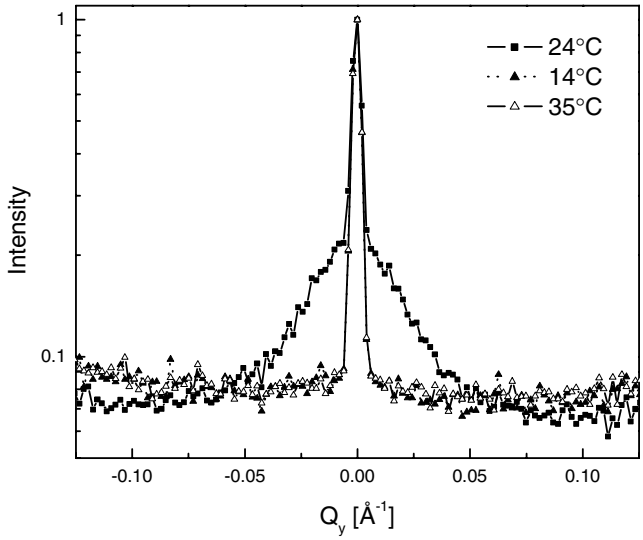

Figure 9. Intensity scans parallel to the solid/liquid interface at fixed $Q_z = 0.0384$ Å^{-1} for three different sample temperatures.

The GISANS experiments confirm that C_8E_4 adsorption at the silica/water interface is a highly cooperative process, with low affinity of the surfactant at low temperature (few isolated molecules), and high affinity at high temperature (uniform adsorption layer, full coverage). Transient clusters with no preferred lateral structure form at the interface at intermediate coverage, i.e., intermediate sample temperature at the chosen bulk concentration (0.8 CMC).

Table 1. Chemical characteristics and asymmetry parameters (β) of the $EO_xPO_yEO_x$ triblock copolymers used in this study.

BAB	Mn	N_{EO}–N_{PO}–N_{EO}	N_A (anchor)	N_B (buoy)	β_{sel}[a]	Company
F108	14 000	122–56–122	28	122	3.37	ICI
F88	10 800	97–39–97	20	97	3.48	ICI
F68	8 400	76–30–76	15	76	3.47	ICI
F127	12 600	100–65–100	33	100	2.76	BASF Corp.
F68	8 400	76–29–76	15	76	3.47	Aldrich
L64	2 900	13–30–13	15	13	1.20	Aldrich

[a] $\beta_{sel} = N_B^{3/5}/N_A^{1/2}$; $\beta_{sel} = 1$, buoy-dominated regime; $\beta_{sel} > 1$, vdW–buoy regime.

4. Amphiphilic triblock copolymers at interfaces

Amphiphilic triblock copolymers of the poly(ethyleneoxide)–poly(propyleneoxide)–poly(ethyleneoxide) family (PEO–PPO–PEO) can be looked at as high-molecular-weight analogues of the C_mE_n surfactants discussed in the previous section. Relevant properties of the polymers used in our studies are summarized in table 1. Like the low-molecular-weight surfactants, PEO–PPO–PEO triblock copolymers are adsorbed to interfaces such as the air/liquid or solid/liquid interface.

4.1. Adsorbed layers at the air/water interface

Neutron reflectivity measurements reveal that a single adsorbed polymer layer is formed at the free surface of dilute aqueous solutions of PEO–PPO–PEO triblock copolymers. The thickness of this layer increases linearly with the chain length of the PEO segments of the polymers, in agreement with the theory of a *simple brush* (see figure 10). The results of the NR experiments are consistent with those of earlier ellipsometric studies which had already indicated the formation of a PEO brush at the air/water interface. The segment density profile was found to be more diffuse than predicted by the *simple brush* model, but the next higher approximation (known as the *parabolic brush*) does not describe our results adequately. For a more detailed discussion on the results the reader is referred to [21]. A similar adsorption behaviour was observed at the hydrophobic solid/liquid interface [22].

4.2. Adsorbed layers at the air/solid interface (after solvent evaporation)

Primary ad-layers. Adsorbed layers of PEO–PPO–PEO triblock copolymers on hydrophilic SiO_x and hydrophobic PS surfaces were studied after solvent evaporation by atomic force microscopy, x-ray reflectivity, ellipsometry and contact angle measurements. These studies revealed that adsorption at the hydrophilic silica surface is dependent in a delicate way on the number of hydrophilic EO and hydrophobic PO groups of the polymer molecule, and the results can be characterized by the asymmetry parameter $\beta_{sel} = N_B^{3/5}/N_A^{1/2}$, where N_B and N_A denote the number of hydrophilic and hydrophobic segments of the molecule, respectively (see table 1). On the hydrophilic silica surface the short-chain polymers L64 ($\beta = 1.2$) and F68 ($\beta = 3.47$) do not form stable layers, but only the polymer F127 (for which the asymmetry parameter has an intermediate value, $\beta = 2.76$) is retained at the surface after extensive rinsing with pure water.

At the hydrophobic PS surface all three polymers, L64, F127 and F68, formed stable adsorption layers. The thicknesses of these layers scaled with the number of EO units in the building blocks. This suggests that the MJL scaling theory [23, 24] can be extended to the dry

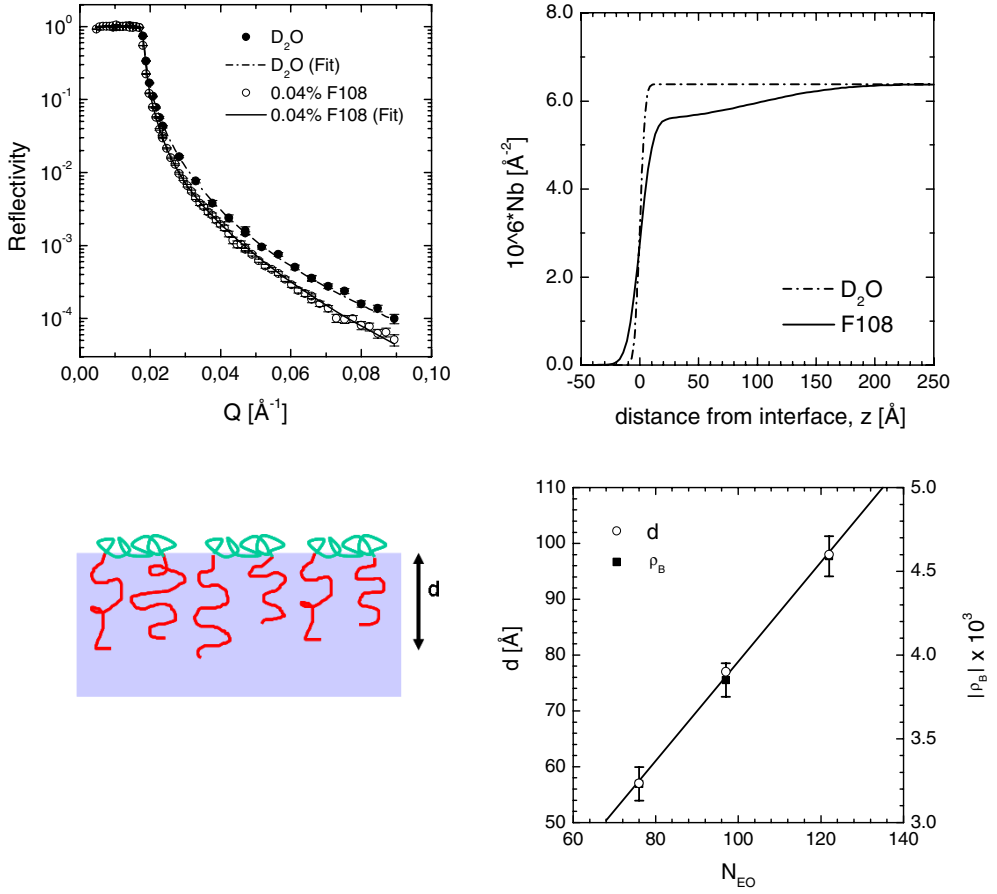

Figure 10. Top left: neutron reflectivity from the free surface of D_2O (solid symbols) and 0.04 wt% F108 in D_2O (open symbols). The solid lines represent the best fits to the data corresponding to the real space profiles plotted on the top right. The thickness, d, of the solvent-swollen polyethyleneoxide part of the adsorption layer (bottom left) scales with the number of EO units, N_{EO}, as shown on the bottom right. For further details see [21]. Reprinted from [21], Copyright (2002), with permission from Elsevier.

state of the collapsed brush after solvent evaporation, at least in this particular case. Together with the observed decrease of the contact angle of water this finding suggests that the EO units of the triblock copolymers are exposed to the environment and that the polymers adsorb with their PPO blocks to the hydrophobic substrate. Hence for F127, where a direct comparison can be made, the ad-layer at the hydrophilic substrate surface is a mirror image of the ad-layer formed at the hydrophobic substrate surface (see figure 11). In all cases the ad-layers gave uniform coating of the substrates on the micron scale with thickness in the nanometre range (1–2.3 nm) suggesting monolayer coverage [25]. These *primary ad-layers* covered the substrates homogeneously. Nanostructured thicker layers of the block copolymers (beyond one monolayer) were observed in the form of *casting layers* deposited on the primary ad-layers when rinsing with pure water was omitted. We believe that those layers are not templated by the first layer adsorbed to the substrate.

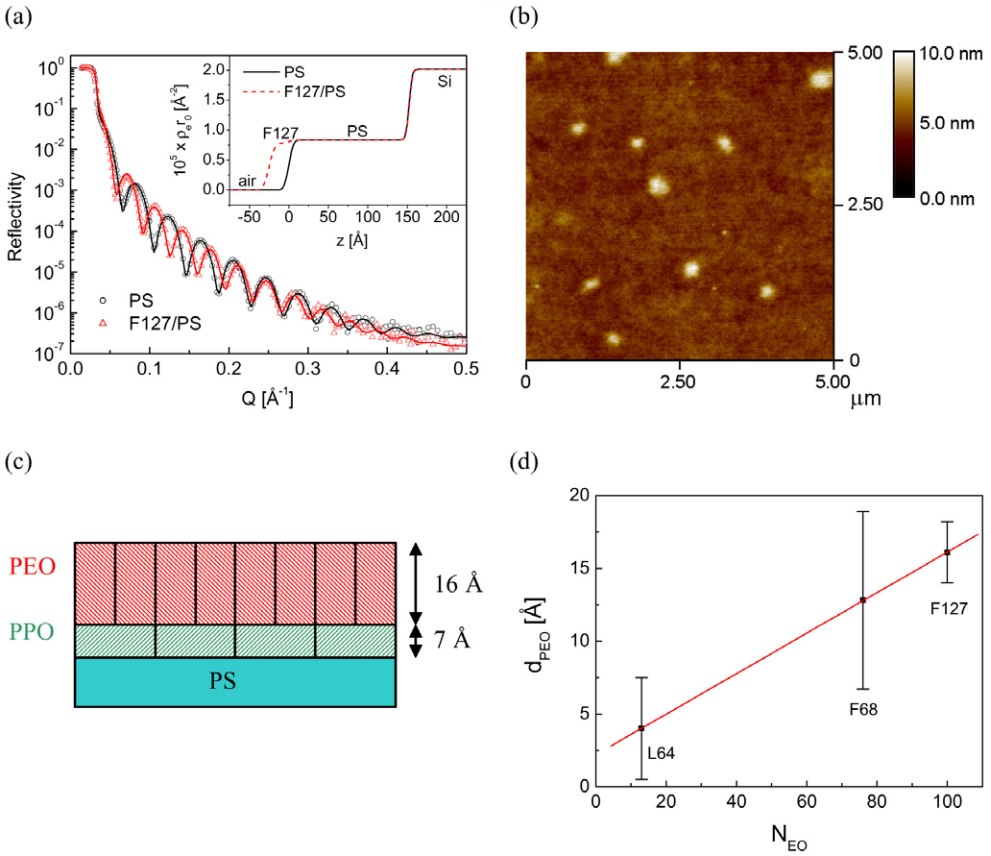

Figure 11. Adsorption of F127 onto a PS coating against air after rinsing with pure water (ten times). (a) X-ray reflectivity from F127 adsorbed to a PS coating. The solid curves represent the best box-model fits to the data (see inset for the real space profiles). (b) AFM topography image recorded in tapping mode from a F127 ad-layer adsorbed at a PS surface. The small hills visible have a height of about 5 nm above the base plane. (c) Schematic diagram of the F127 ad-layer as retained on the hydrophobic PS surface. Excess material as seen by AFM (top right) forms a second lamella of 5 nm height (casting layer with incomplete coverage) on top of the ad-layer on the hydrophobic surface (not shown). (d) Thickness of the PEO blocks, d_{PEO}, plotted versus the PEO chain length, i.e. number of EO segments, N_{EO}, for the different triblock copolymers investigated. For details see [25]. (b) and (d) reprinted from [25], Copyright (2004), with permission from Elsevier.

Results for casting layers. Investigation of the casting layers by AFM showed lamellar structures of dendritic or spinodal morphology after adsorption of the triblock copolymer from very dilute solution below the critical micelle concentration (CMC) on both silica and polystyrene surfaces. Increased concentration around and above the CMC induced nanoscale micelles of uniform size (50 nm in-plane (x–y) dimensions and 5 nm thickness). As opposed to the primary adsorption layers the surface structures of the casting layers are dependent on solution concentration rather than being determined by the chemical nature of the substrate [26].

Figure 12 shows a series of AFM topographic images of films deposited at the surface of a hydrophilic silicon wafer from F127 triblock copolymer solutions of different concentrations. The freshly cleaned silicon substrates were dipped into different polymer solutions (below and above the CMC) and kept there for 1 h to allow for equilibrium adsorption. For very

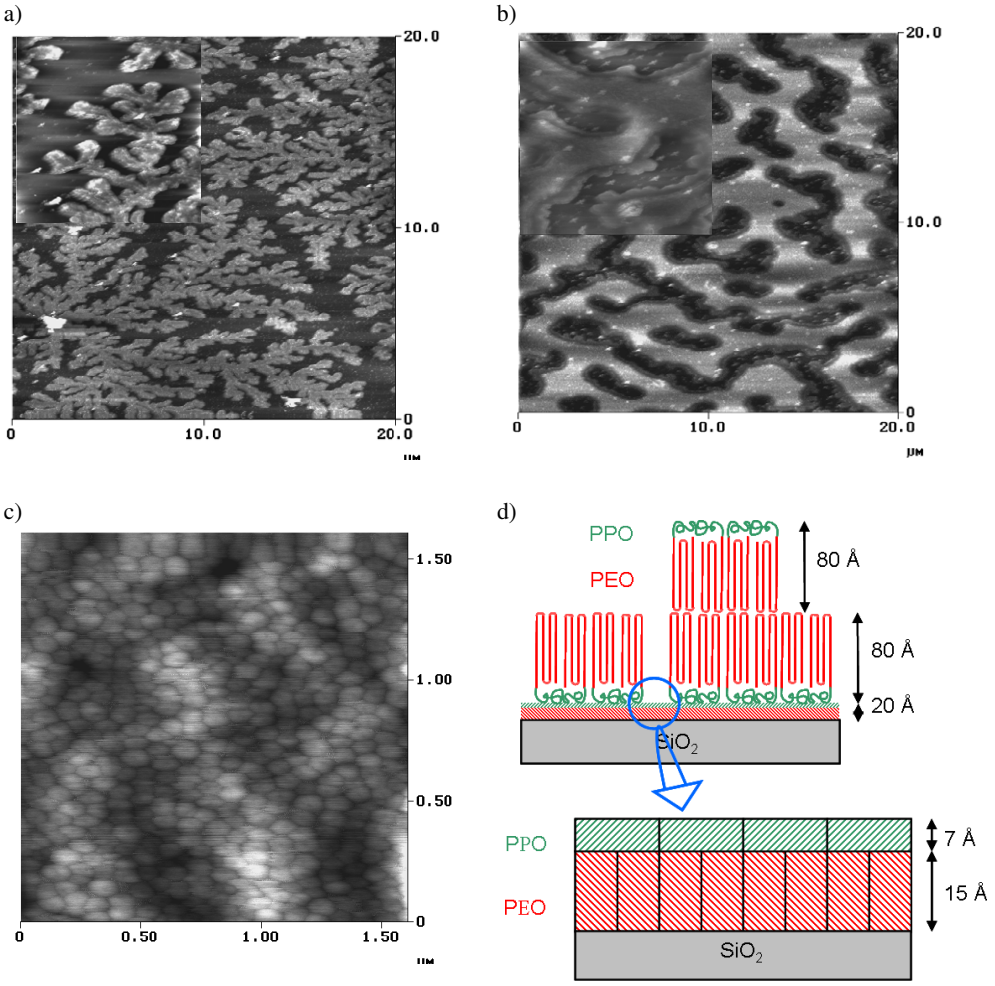

Figure 12. Morphology changes of F127 casting layers on silica substrates as a function of copolymer concentration of the dipping solution. AFM topography images recorded in tapping mode after solvent evaporation from (a) 0.1 wt%, (b) 0.3 wt% and (c) 3 wt% aqueous solution (about 3 CMC). The insets in the top left of (a) and (b) are zoomed-in areas. They show that the adsorbed F127 forms distinct terraces. (d) A schematic diagram of the proposed molecular organization of the casting layers (top) shown in (a) and (b) on top of the underlying primary adsorption layer (bottom).

dilute solutions, dendritic lamellae of uniform height were observed, as shown in figure 12(a). Zooming in reveals a bilayer-type organization with the lamellae aligned parallel to the substrate surface. Two terraces can be seen where the top layer exactly reproduces the borderlines of the bottom layer. The surface is not completely covered by the triblock copolymer. Cross-sectional profile analysis of the lamellae in the height image indicates that the adsorbed layer thickness is approximately 8 nm. Similar observations have been reported for spin-coated PEO homopolymer films after annealing [27, 28]. It is reasonable to assume that dendritic lamellar bilayers are formed on top of pre-adsorbed polymer brushes [23, 29]. The underlying polymer brushes are very thin: about 2.3 nm. Increasing the triblock copolymer concentration (0.3 wt%) yielded lamellar multilayers with tortuous island/hole patterns, again of uniform

height (figure 12(b)). At this concentration, two terraces can be seen where the top layer exactly reproduces the borderlines of the bottom layer, yet indented by a distinct offset (see the inset in figure 12(b)). Cross-sectional profile analysis of the multilayers showed that the height of each lamellar layer is about 8 nm, the same as the height of the dendritic lamellar layer. Upon further increase of the solution concentration to 1 wt% (about the CMC) nanoscale uniform surface micelles with lateral diameter of about 50 nm formed (not shown). The micellar coverage of the surface is not complete, and the height of surface micelles was found to be 2–5 nm from the cross-sectional profile analysis. Apparently, the surface micelles collapse during solvent evaporation and tip scanning. Films adsorbed from even higher concentration (above 3 wt%) induce a dense packing of such micelles, which completely covers the surface. Figure 12(c) shows a very smooth surface consisting of uniform micelles. Within the layer the micelles tend to arrange in hexagonal order. The AFM picture shows black dots in the centre of surface micelles as the originally spherical micelles are collapsed after solvent evaporation and deformed to hexagonal shape. Similar results have been reported for a diblock copolymer system [30]. It was found that the deformed micelles were stable for weeks at room temperature. We did not observe further morphologies or morphological changes upon further increasing the concentration of the polymer solution.

The spontaneous self-assembly of F127 triblock copolymers into surface micelles is qualitatively similar to the behaviour of diblock copolymers, which were explained in terms of balancing the conformational free energy at the interface [31, 32]. A similar mechanism seems to be the driving force in the thin films reported here. However, dendritic bilayers and spinodal-type multilayers formed from dip-coating after solvent evaporation seem to be similar to the structures observed for spin-coated PEO homopolymer films after isothermal crystallization [27] and therefore were investigated in further detail [26].

5. Summary and outlook

This work has been concerned with boundary layers of aqueous surfactant systems at solid/liquid interfaces, with special emphasis on effects induced by the hydrophobicity of the substrate surface in the boundary layer of the aqueous phase. The investigations on the molecular and mesoscopic length scale revealed that the hydrophobicity of the substrate surface has a strong influence on the wetting properties of the water phase. A pronounced depletion of water was found, amounting to about 10% of the bulk density in about 3 nm thickness, at the interface of hydrophobic deuterated polystyrene against D_2O ($\theta_w = 90°$). This depletion layer is seen as the precursor of the nanobubbles as observed by AFM at this interface and at related interfaces by other groups and is indicative of a weak dewetting at hydrophobic solid/liquid interfaces. No such depletion was observed in the boundary layer of water against more hydrophilic polymers (polyelectrolyte/water interfaces with $\theta_w \leqslant 63°$).

The adsorption of the low-molecular-weight nonionic surfactants $C_{10}E_4$ and C_8E_4 improves the wettability of the substrates by the aqueous phase, even at surfactant concentrations well below the CMC. Different morphologies of the adsorption layers are formed depending on the architecture of the surfactant molecules at otherwise identical interfaces. The water content in the adsorption layers is very high ($\sim$30% by volume), even in the condensed layers. GISANS experiments conducted on the system $SiO_2/C_8E_4/D_2O$ revealed that no periodically ordered structures (such as a uniform distribution of surface micelles) are formed at the interface. However, the experiments prove the existence of transient adsorbed surfactant clusters (presumably bilayer patches) at the hydrophilic solid/liquid interface.

Replacing the low-molecular-weight nonionic surfactants by their high-molecular-weight analogues, PEO–PPO–PEO triblock copolymers, introduces additional features. In particular,

in the case of thicker films of F127, surface patterning on the mesoscopic length scale is observed after solvent evaporation. Adsorption to the air/liquid and the solid/liquid interface under equilibrium conditions leads to the formation of a solvent-swollen brush, which transforms to a uniform and dense coating of the underlying substrate by the triblock copolymer after extensive rinsing with pure water and subsequent solvent evaporation. This primary adsorption layer retains properties of the precursor brush. In particular, its thickness scales with the number of EO units of the chosen polymer. Surface patterning starts on top of the primary ad-layer as a function of the total amount of the triblock copolymer available upon drying without rinsing. We conclude that this surface patterning is mainly driven by segregation forces within the casting layers and not by interactions between the layer and the substrate, as similar patterns are found on bare silicon and PS-coated silicon substrates.

The present brief review of recent work is far from complete. It points out that further work has to be conducted to achieve a better understanding on the driving forces of the observed pattern formation of triblock copolymers on homopolymer substrates. Of equal significance is the findings on the boundary layer of water at the plain polymer/liquid interface, which has already invoked new theoretical studies [33] and further experimental work, in order to gain a better understanding of the phenomena related to wetting on the molecular and the mesoscopic length scale.

Acknowledgments

The authors thank J Howse, S Zhang, S Uredat and D Akcakayiran for valuable contributions to this work. Financial support of the Deutsche Forschungsgemeinschaft through the priority programme SPP 1052 (grant FI 235/13) is gratefully acknowledged.

References

[1] Steitz R, Gutberlet T, Hauß T, Klösgen B, Krastev R, Schemmel S, Simonsen A C and Findenegg G H 2003 *Langmuir* **19** 2409–18
[2] Tyrrell J W G and Attard P 2001 *Phys. Rev. Lett.* **87** 176104
[3] Jensen T R, Østergaard Jensen M, Reitzel N, Balashev K, Peters G H, Kjaer K and Bjørnholm T 2003 *Phys. Rev. Lett.* **90** 086101
[4] Schwendel D, Hayashi T, Steitz R, Schreiber F, Dahint R, Pertsin A and Grunze M 2003 *Langmuir* **19** 2284–93
[5] Lum K, Chandler D and Weeks J D 1999 *J. Phys. Chem.* B **103** 4570 and references given in this article
[6] Ishida N, Kinoshita N, Miyahara M and Higashitani K 1999 *J. Colloid Interface Sci.* **216** 387–93
[7] For details on the preparation see: Decher G 1997 *Science* **277** 1232
[8] Loesche M, Schmitt J, Decher G, Bouwman W G and Kjaer K 1998 *Macromolecules* **31** 8893
[9] Steitz R, Leiner V, Siebrecht R and Klitzing R v 2000 *Colloids Surf.* A **163** 63
[10] Gilchrist V A, Lu J R, Staples E, Garett P and Penfold J 1999 *Langmuir* **15** 250
[11] Russell T P 1990 *Mater. Sci. Rep.* **5** 171
[12] Howse J, Steitz R, Pannek M, Simon P, Schubert D W and Findenegg G H 2001 *Phys. Chem. Chem. Phys.* **3** 4044–51
[13] Király Z, Börner R H and Findenegg G H 1997 *Langmuir* **13** 3308
[14] Corti M, Minero C and Degiorgo V 1984 *J. Phys. Chem.* **88** 309
[15] Schemmel S, Howse J, Steitz R, Uredat S and Findenegg G H 2004 Surfactant adsorption layers at polymer-solution interfaces. A neutron reflectivity study (Manuscript in preparation)
[16] Stålgren J J R, Eriksson J and Boschkova K 2002 *J. Colloid Interface Sci.* **253** 190–5
[17] Müller-Buschbaum P, Gutmann J S, Stamm M, Cubitt R, Cunis S, Krosigk G v, Gehrke R and Petry W 2000 *Physica* B **283** 53
[18] Steitz R, Müller-Buschbaum P, Schemmel S, Cubitt R and Findenegg G H 2004 *Europhys. Lett.* **67** 962
[19] Findenegg G H, Braun Ch, Lang P and Steitz R 1999 *Supramolecular Structure in Confined Geometries* (*ACS Symp. Series* vol 736) ed S Manne and G G Warr (Washington, DC: American Chemical Society) p 24ff

[20] Howse J R, Manzanares-Papayanopolous E, McLure I A, Bowers J, Steitz R and Findenegg G H 2002 *J. Chem. Phys.* **116** 7177
[21] Sedev R, Steitz R and Findenegg G H 2002 *Physica* B **315** 267–72
[22] Sedev R, Schemmel S and Steitz R 2002 *PEO–PPO–PEO Triblock Copolymers at the Polymer/Water Interface, BENSC Experimental Report 2002* http://www.hmi.de/bensc/report2002/pdf-files/164_PHY-04-0732.pdf
[23] Marques C, Joanny J F and Leibler L 1988 *Macromolecules* **21** 1051
[24] Joanny J F 1989 *Macromolecules* **22** 1454
[25] Shi H, Zhang S, Steitz R, Cheng J, Uredat S and Findenegg G H 2004 *Colloids Surf.* A **246** 81
[26] Shi H, Zhang S, Steitz R and Findenegg G H 2004 Microstructured coatings of a triblock copolymer (Manuscript in preparation)
[27] Reiter G and Sommer J-U 2000 *J. Chem. Phys.* **112** 4376
[28] Reiter G, Castelein G and Sommer J-U 2001 *Phys. Rev. Lett.* **86** 5918
[29] Guzonas D, Hair M L and Boils D 1991 *Macromolecules* **24** 3383
[30] Spatz J P, Sheiko S and Moller M 1996 *Macromolecules* **29** 3220
[31] Hashimoto T 1991 *Macromolecules* **24** 240
[32] Shull K R 1993 *Macromolecules* **26** 1346
[33] Mamatkulov S I, Khabibullaev P K and Netz R R 2004 *Langmuir* **20** 4756–63